Optimal Design and Management of a Hybrid Energy Storage System

Eugene Kim and Kang G. Shin
{kimsun,kgshin}@umich.edu

***Abstract*— Electric Vehicles (EVs) are powered by a large number of battery cells, which must be managed effectively/efficiently to deliver the required power/energy during their warranty period. An EV's operation requires large and fluctuating power from its battery pack, but its battery cells have only limited tolerance to (dis)charge stress, accelerating their degradation. Moreover, battery cells have different (dis)charge stresses depending on their physical positions in the battery pack, causing different degradation rates and thus the unbalanced State-of-Health (SoH) or State-of-Charge (SoC). To address this problem, we design, implement and evaluate a novel energy storage system with energy buffers and an SoC-balancing circuit, to extend both the battery life and EV's operation-time. We first design a hybrid energy storage system that efficiently meets the EV's representative power requirement. We then develop an optimal power distribution to minimize the EV's energy consumption and its battery cells' stress. We prototyped and evaluated this solution, demonstrating a reduction of discharge/charge stress by about 21.8%, and thus extending battery lifetime while balancing cells' SoC.**

I. Introduction

Electric Vehicles (EVs) require high voltage and high current to power their motors. So, an EV's battery pack usually contains hundreds of small cylindrical battery cells or a few large battery pouches connected in parallel to supply high current, and a large number of these battery cells/pouches connected in parallel which are then connected in series to form a high-voltage power source.

EVs' batteries must support large peak (dis)charge currents to (i) power the high electric loads needed during acceleration and/or hill climbing, and (ii) accommodate the momentary power generated during regenerative breaking. The resultant current surges of batteries cause extensive energy dissipation and hence heating, accelerating batteries' capacity degradation. To mitigate these (dis)charge/charge surges, researchers proposed hierarchical energy-storage systems consisting of a main energy storage (i.e., a battery pack) with high energy-density and a high power-density energy buffer [1–4]: the former extends the driving range, while the latter enables quick acceleration and accommodates momentary power generated during regenerative braking. Such a hierarchical energy-storage system reduces the number of battery cells needed to provide the required peak currents while reducing the cost of battery pack.

Another issue of large battery packs is the imbalance of their cells' State-of-Charge (SoC). In a pack with serially-connected battery cells, the same current flows through every battery cell in the pack even when their energy capacity and SoC are different. This causes incomplete (dis)charging of the battery pack to protect battery cells from over-charging and/or deep-discharging. Various cell-balancing techniques have been proposed to make the energy stored in all battery cells even [5]. *Active cell balancing* mitigates the energy loss of passive balancing by redistributing energy from cells with higher SoCs to those with lower SoCs using an inductive or capacitive energy storage.

Battery packs must be managed effectively to handle their battery cells' imbalance and peak (dis)charge currents. The battery management system (BMS) must transfer energy not only among the battery cells to balance their SoCs, but also between the battery pack and the energy buffer to reduce peak current surges. While hardware architectures and control algorithms have been proposed to efficiently transfer charges for balancing cells and reducing the peak power requirements, little has been done on how they can be optimized and effectively applied in real operating environments. A dynamic programming (DP) approach has been proposed in [3] to derive the best hybrid energy storage system (HESS) configuration and discharge/charge currents. However, it is difficult to apply this approach in practice because it requires fixed/known driving cycles and DP programming to find parameters for its rule-based strategy. It did not cover SoC-balancing either.

To fill this gap, we propose the design and management of a HESS that can be used in realistic settings without prior knowledge of power requirements while balancing cells' SoC. We first determine the optimal sizes of the energy-dense main battery and power-dense energy buffer to effectively reduce the peak power and also to balance cells' SoC. We then adaptively determine the (dis)charge current of the battery pack and the energy buffer based on the historical power requirements and the SoC of different energy components, thus supplying the required power while balancing battery cells' SoC without any pre-tuned parameters for control rules.

II. Background and Overall Approach

This section provides the background and presents our architecture for power management. Fig. 1 shows a HESS consisting of energy-dense batteries and energy buffer. It requires a DC/DC voltage converter since each energy source has a distinct terminal voltage. Our proposed approach optimizes the sizes of energy-dense and power-dense components, and determines the desired (dis)charge power of the components.

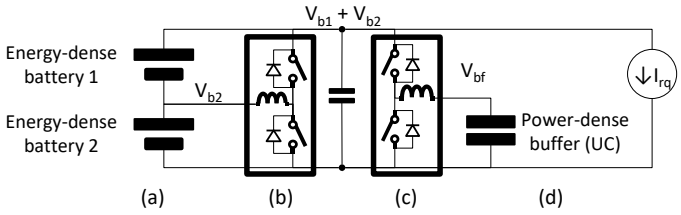

Fig. 1. The BMS architecture under consideration consisting of (a) energy-dense batteries, (b) a voltage converter between stacked batteries ($V_{b1}+V_{b2}$) and one battery (V_{b2}), (c) a voltage converter between stacked batteries' voltage ($V_{b1}+V_{b2}$) and buffer voltage (V_{bf}), and (d) a power-dense buffer for peak power reduction.

A. Hybrid energy storage system for powering vehicles

Energy capacity, E, and power capability, P, are two of the most representative performance metrics for an energy storage system. Specific energy (power) is the amount of energy (Wh) (maximum power (W)) that the energy storage can provide per unit mass (kg). Usually, there is a tradeoff between the specific energy and power, depending on their design as shown in Fig. 2. For example, in a Li-ion battery cell, increasing active materials density improves the specific energy E^s (Wh/kg) because of more available Li-ion sites. However, it also reduces the specific power P^s (W/kg) due to the reduced paths for Li-ion to transport. Therefore, battery cell/pack designers must choose cell performance (P^s, E^s) and their sizes, m_{rq} (kg) based on the power/energy requirements ($P = m_{rq}P^s$, $E = m_{rq}E^s$) of the targeted applications. For example, to build a battery pack with 85 kWh energy capacity and 278 kW of power capacity, we could design 650 kg of batteries with 131 Wh/kg specific energy and 428 W/kg power.

In a hybrid energy storage system (HESS), multiple energy storage options can provide more energy/power without increasing total system size. For instance, we can develop a higher performance battery pack using (i) 629 kg of a battery whose specific energy is 155 Wh/kg and specific power is 100 W/kg, and (ii) 21 kg of a different battery whose specific energy is 40 Wh/kg and power is 10,000 W/kg. This battery configuration has 98,335 Wh of energy capacity and 272,900 W of power capability for 14.4 seconds. Note that how long the battery can supply its full power depends on specific power/energy ($= \frac{E^s(Wh/kg)\cdot s/h}{P^s(W/kg)} = \frac{40\times 3{,}600}{10{,}000} = 14.4\ s$). This battery pack stores 16% more energy than the above pack consisting of a single battery type, while maintaining the comparable power capability for short bursts of peak (dis)charge current.

B. The proposed approach

We propose a framework that optimizes the storage sizes in HESS and adjust power distribution from each storage to maximize the system performance. Fig. 2 shows an overview of the HESS design and power management. Energy- and power-dense batteries in a HESS must be sized to supply sufficient power to the electric load as long as possible. Meanwhile, we must consider design constraints such as the total weight, the required power capability, and the energy capacity for powering vehicles. The algorithm determines

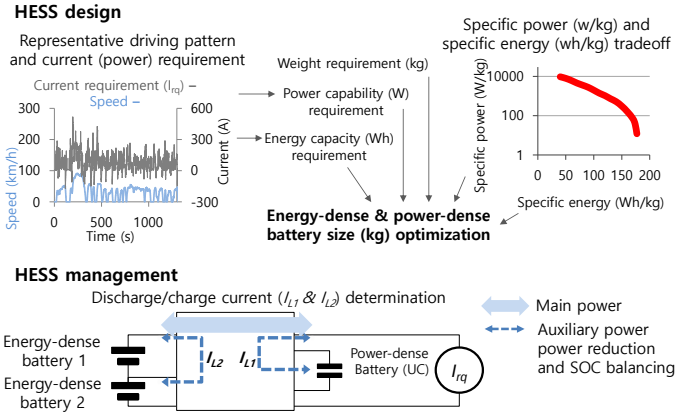

Fig. 2. Overview of the proposed HESS design and its management.

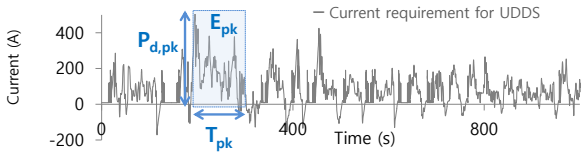

Fig. 3. Peak power and energy of a representative driving pattern provided by US Environmental Protection Agency (EPA) [6].

effective discharge/charge current from each battery based on cells' SoCs, and the current requirement pattern.

III. Design of a HESS with Power- and Energy-Dense Batteries

We first analyze the required power/energy capacities of a HESS, and then make a formal statement of the HESS design problem subject to these constraints.

A. Power requirement analysis and HESS requirements

In the HESS architecture, the energy-dense battery must be able to supply at least the average required power (P_{avg}) of the electric load, and the power-dense battery must be able to accommodate the surplus energy and supply the energy to the electric load when the peak power is required. These requirements indicate the energy capacity of the power-dense battery must be larger than the energy that could be charged into the power-dense battery or discharged to the electric load during peak charge/discharge periods. We identify the peak discharge/charge powers ($P_{d,pk}, P_{c,pk}$) during a given time duration (T_{pk}) in the power demand profiles. Note that this time duration (T_{pk}) must cover at least one discharge/charge burst period to capture the power requirement pattern as illustrated in Fig. 3. These parameters affect the energy capacity specification of power-dense battery:

$$E_{pk} = T_{pk} \cdot P_{d,pk}$$

B. Design of HESS

With the above design requirements, our problem can be formally stated as:

Given the weight requirement (m_{rq}), and a tradeoff function (f_{ep}) between the specific power (P^s) and energy (E^s),

Optimize the HESS design parameters $\{E_e^s, m_e, E_p^s, m_p\}$ to

$$\begin{aligned}
&\text{maximize (S0)} && \text{HESS energy capacity} = E_e^s \cdot m_e + E_p^s \cdot m_p \\
&\text{subject to (S1)} && P_e^s \cdot m_e + P_p^s \cdot m_p \geq P_{pk} \\
&\text{(S2)} && E_p^s \cdot m_p \geq E_{pk} \\
&\text{(S3)} && P_e^s \cdot m_e \geq P_{avg} \\
&\text{(S4)} && m_e + m_p = m_{rq}, \qquad (1)
\end{aligned}$$

where E_e^s is the specific energy of the energy-dense battery, m_e the weight of the energy-dense battery, E_p^s the specific energy of the power-dense battery, m_p the weight of the power-dense battery, and m_{rq} the total maximum weight requirement. P_e^s and P_p^s are the specific powers of the energy-dense battery and power-dense battery, respectively, and they can be determined by their specific energy ($P_e^s = f_{ep}(E_e^s), P_p^s = f_{ep}(E_p^s)$). To make the problem analytically solvable, we assume that the system cost depends only on the weight, and approximate the tradeoff between Li-ion battery power capability and energy capacity ($P^s = f_{ep}(E^s)$) based on the recent result reported in [7]. The objective function in (S0) represents the total energy capacity of the HESS, which should be maximized while ensuring the battery system to supply the peak power (S1). To support the system's peak power, the power-dense battery must have a sufficient energy capacity to be able to supply the peak power (S2). Also, the energy-dense battery, as the primary energy source, should be able to provide the average required power to the load (S3). Last but not the least, the total weights of the energy storage components (m_e+m_p) must be lower than the weight limit (m_{rq}) (S4).

IV. (Dis)charge Management for Peak Power Reduction and SoC Balancing

Thus far, we have explored the HESS design to maximize system performance based on the underlying power requirements. Next we develop algorithms to determine the (dis)charge currents of the batteries in the HESS. These algorithms should consider the current requirement pattern (I_{rq}) and SoC (z) of each energy storage component for the efficient management. Alg. 1 describes the overall discharge/charge current management for peak power reduction and SoC balancing. Alg. 2 periodically calculates the effective current bounds that Alg. 1 needs.

A. Problem statement

We can formally state the problem as:

Given the power requirement (I_{rq}), a set of battery SoCs and the performance parameters of energy storage components,

Determine the (dis)charge currents from energy components $\{I_{L_1}[k],\ I_{L_2}[k]\}_{0<k<k_e}$, such that

$$\begin{aligned}
&\text{Minimize (S5)} && \text{Dischage/charge stress} = \frac{1}{T_{op}} \int a \cdot e^{b \cdot |I_b|}\ dt \\
&\text{Subject to (S6)} && I_{rq} = I_{L_1} + I_{L_2} + I_b \\
&\text{(S7)} && z_1[k_e] = z_2[k_e]. \qquad (2)
\end{aligned}$$

Algorithm 1 Target current decision (I_{L_1}, I_{L_2})

```
1: while 1 do
2:     if I_{b,ub} < I_{rq,n} then    /* Peak power reduction */
3:         I_{L_1} ← I_{rq} − I_{b,ub}
4:     else if I_{b,lb} > I_{rq,n} then
5:         I_{L_1} ← I_{rq} − I_{b,lb}
6:     else
7:         I_{L_1} ← 0
8:     end if
9:     if Δz > Δz_{st} then       /* Target current for SoC balancing */
10:        while Δz > Δz_{end} do
11:            if I_{z,ub} > I_{rq,n} > I_{z,lb} then
12:                I_{L_2} ← min(I_{z,ub} − I_{rq}, I_{rq} − I_{z,lb})
13:                if z_1 > z_2 then
14:                    I_{L_2} ← −I_{L_2}
15:                end if
16:            else
17:                I_{L_2} ← 0
18:            end if
19:        end while
20:    else
21:        I_{L_2} ← 0
22:    end if
23: end while
```

The energy storage system must supply the required power with current (I_{rq}) to the electric load. As energy conserves, the sum of current supplies from energy storage components (I_{L_1}, I_{L_2}, I_b) must be the power requirement for all $k \in [0, k_e)$ (S6). Also, the current flows between batteries must be controlled to balance their SoC (S7). The objective function in (S5) captures the (dis)charge stress during an operation period of T_{op}. We assume the (dis)charge stress to be exponential with the (dis)charge current, because large (dis)charge current exponentially accelerates the battery degradation by exciting high over-potential between solid-phase and solution-phase voltages [8].

B. Overall algorithm

Alg. 1, Figs. 4–6 show our overall algorithm. Lines 2–8 of Alg. 1 determine the discharge current from the power-dense battery (I_{L_1}) to meet the high (dis)charge current requirement (I_{rq}). When I_{rq} is greater than its upper bound ($I_{b,ub}$), the power-dense battery provides energy to reduce the discharge current of the energy-dense battery (lines 2–3). When I_{rq} is less than its lower bound ($I_{b,lb}$), the power-dense battery takes in the generated current to protect the energy-dense battery from over-recharge current (lines 4–5). The algorithm also determines the target current between the energy-dense batteries (I_{L_2}) to balance the battery cells' SoCs (lines 9–22). If the SoC difference (Δz) is larger than a pre-defined threshold (Δz_{st}), the SoC-balancing kicks in until Δz reduces to the termination condition (Δz_{end}). The balancing operation transfers the charge in a battery with higher SoC to the one with lower SoC (lines 13–14), and the balancing current is limited to protect the energy-dense batteries from over-(dis)charge current (lines 12). For both power buffering and SoC-balancing, current upper/lower bounds are critical because they dictate the amount of dis(charge) current of the storages. Next, we describe how to determine the current bounds.

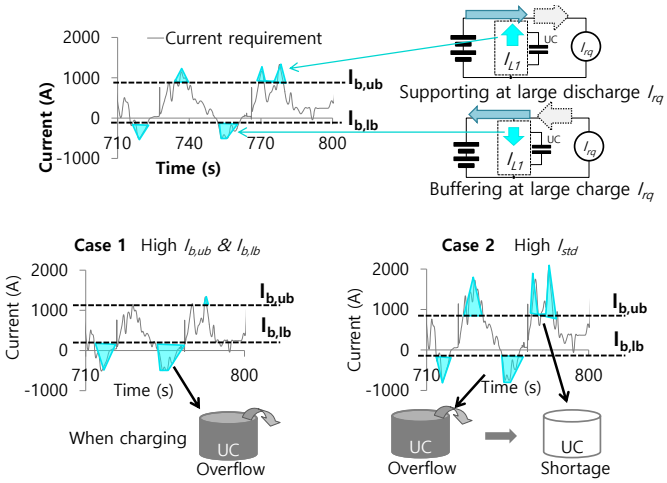

Fig. 4. Example of power buffering for reduction of peak power. Case 1 shows the UC state during charging and discharging if $I_{b,ub}$ and $I_{b,lb}$ are high. Large current bounds limit the discharging current from UC and increase the charging current to UC. Case 2 shows the UC state if actual peak currents are higher (and so I_{std} is higher). Higher dis(charge) currents cause larger dis(charge) current from UC, leading to more frequent UC overflow/shortages

Algorithm 2 Determination of the current bounds for peak current reduction and SoC-balancing

1: $E_c \leftarrow \frac{1}{2} C_c V_{c,rated}^2$
2: **while** 1 **do**
3: $T_c \leftarrow$ DisChargeCycleTimeUpdate()
4: $I_{avg}[k] \leftarrow \frac{k-1}{k} I_{avg}[k-1] + \frac{1}{k} I_{rq}$
5: $I_{std}[k] \leftarrow \{\frac{k-1}{k} I_{std}[k-1]^2 + \frac{1}{k}(I_{rq} - I_{avg}[k])^2\}^{\frac{1}{2}}$
6: $[I_{ub}, I_{lb}] \leftarrow$ FindBound($T_c, E_c, I_{avg}[k], I_{std}[k]$)
7: $I_{b,ub} \leftarrow I_{avg}[k] + (I_{ub} - I_{lb})(1 - (z_c[k] - z_c^{opt}))$
8: $I_{b,lb} \leftarrow I_{avg}[k] - (I_{ub} - I_{lb})(1 - (z_c^{opt} - z_c[k]))$
9: $E_z \leftarrow |E_{bat_1}(z_{b_1}) - E_{bat_2}(z_{b_2})|$
10: $T_z \leftarrow$ TargetBalanceTimeUpdate()
11: $[I_{z,ub}, I_{z,lb}] \leftarrow$ FindBoundSOC($T_z, E_z, I_{avg}[k], I_{std}[k]$)
12: Sleep()
13: **end while**

C. Determination of current bounds

This section describes how to determine the current bounds ($I_{b,ub}$, $I_{b,lb}$, $I_{b,ub}$ and $I_{b,lb}$). Alg. 2 is the main core that consists of two bound searching algorithms and their preparation steps.

1) Power requirement pattern and power-dense battery capacity (lines 1–6): The amount of required energy depends on the driving pattern, motor performance, and regenerative braking system (RBS), introducing an uncertainty in the amount of required discharge/charge current during driving. To handle this uncertainty, the algorithm calculates the average and standard deviation of the required current ($I_{avg}[k]$, $I_{std}[k]$). Then, the current bound are determined under the assumption that the required current would follow a Gaussian normal distribution with average, I_{avg}, and standard deviation, I_{std}. When the average required current(I_{avg}) is high, the current bounds I_{ub} and I_{lb} should be increased to effectively buffer recharging energy and supply the energy while limiting the energy-dense battery discharge/charge current as shown in Fig. 4. The standard deviation of the required current (I_{std}) also affects the determination of I_{ub} and I_{lb}. A large standard deviation means the transfer of a large amount of energy with a high peak current. In such a case, I_{ub} should be increased and I_{lb} decreased to buffer energy effectively without incurring shortage of energy in the power-sense battery as shown in Fig. 4.

Algorithm 3 FindBound

1: **procedure** $[I_{ub}, I_{lb}]$ = FINDBOUND(E_c, I_{avg}, I_{std})
2: **for** $I_{ub} = I_{avg}; I_{ub} < I_{avg} + 2I_{std}; I_{ub} = I_{ub} + \frac{I_{std}}{20}$ **do**
3: **if** $E_{bf}(I_{ub}) > E_c$ **then**
4: *Break*;
5: **end if**
6: **end for**
7: $I_{lb} = I_{avg} - (I_{ub} - I_{avg})$
8: **return** $[I_{ub}, I_{lb}]$
9: **end procedure**

Alg. 3 and Fig. 5 describe how to determine I_{ub} and I_{lb} for peak power reduction based on the energy capacity and the history of required current. During the charging/recharging cycle (T_c), the power-dense battery buffer receives power from the electric load and supplies power to the load once. To maximize the utilization of power-dense battery buffer, when it is recharging, it must be charged as much as possible without overcharging. Also, it should use most of stored energy during the discharging period. That is, I_{ub} and I_{lb} should be set to make the buffered energy (E_{bf}) equal to the buffer energy capacity (E_c). The energy stored in the battery (E_c) can be calculated based on the voltage level. For example, if we use a ultra-capacitor (UC) as the power-dense battery, we can use the standard equation related to the capacitor energy ($E_c = \frac{1}{2} C_c V_{c,rated}^2$), where $V_{c,rated}$ is UC-rated voltage and C_c UC capacitance. To estimate the amount of the buffered energy in UC (E_{bf}), we assume that current requirement patterns follow a Gaussian distribution with average (I_{avg}) and standard deviation (I_{std}) of the required current. We can then probabilistically calculate the amount of the buffered energy (E_{bf}) by integrating buffered current ($I_{bf} = i - I_{ub}$) as:

$$
\begin{aligned}
E_{bf}(I_{ub}) &= \int_0^{T_c} P_{bf}(t)dt = T_c \int_{I_{ub}}^{\infty} P_{bf}(i)\mathrm{PDF}(i)di \\
&= T_c \int_{I_{ub}}^{\infty} V_b I_{bf}(i)\mathrm{PDF}(i)di \\
&= T_c \int_{I_{ub}}^{\infty} V_b (i - I_{ub})\mathrm{PDF}(i)di \\
&= T_c V_o \Big[\int_{I_{ub}}^{\infty} i\mathrm{PDF}(i)di - I_{ub} \int_{I_{ub}}^{\infty} \mathrm{PDF}(i)di \Big] \\
&= T_c V_o \Big[\int_{I_{ub}}^{\infty} i\mathrm{PDF}(i)di - I_{ub}(1 - \mathrm{CDF}(I_{ub})) \Big] \\
&= T_c V_o \Big[I_{std}^2 \mathrm{PDF}(I_{ub}) + (I_{avg} - I_{ub})(1 - \mathrm{CDF}(I_{ub})) \Big],
\end{aligned}
\tag{3}
$$

where V_o is the battery output voltage, and P_{bf} is the buffered power.

2) Buffer State-of-Charge (lines 7–8): We assume that the power requirement follows a Gaussian distribution, but this assumption is unlikely to hold for the power requirement during every period. Lines 7–8 additionally adjust the upper and

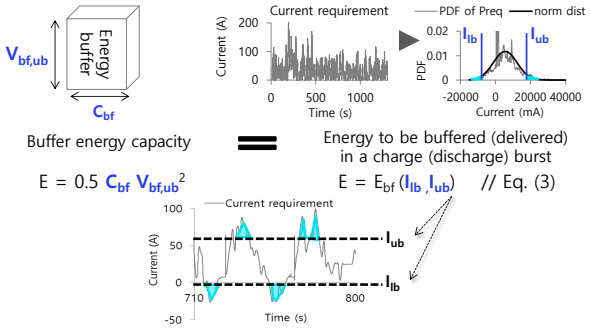

Fig. 5. Determination of current bounds for peak power reduction

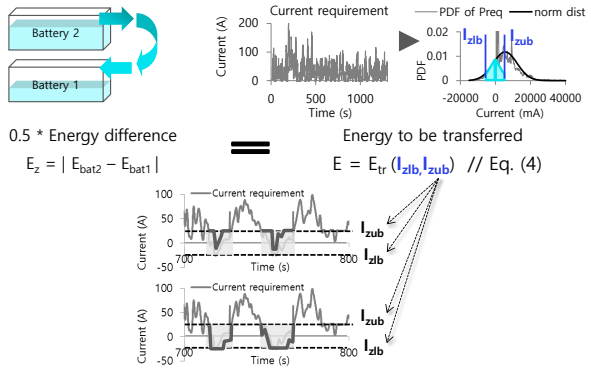

Fig. 6. Determination of current bounds for SoC-balancing

lower current bounds based on the SoC of the power-dense battery, protecting the battery in case the required current is larger than expected. When the power-dense battery is fully charged ($z_c \approx 100\%$), it cannot be charged any more. Therefore, when z_c is high, we need to decrease I_{lb} to reduce the charging energy, and decrease I_{ub} to use more energy in it to support the load. When it is discharged fully ($z_c \approx 0\%$), it cannot be discharged any more. Therefore, when z_c is low, we need to increase I_{lb} and decrease I_{ub}.

3) Power requirement pattern and SoC-balancing (lines 9–11): Currents between batteries also have to be regulated for SoC-balancing based on the total required current (I_{rq}). When battery supplies large power to the load, or receive power from the load, additional current for SoC-balancing may harm the battery's health. Therefore, we determine an acceptable range of the required current for cell balancing to protect cells from over-discharge/charge currents. The current bounds for SoC operation ($I_{z,ub}, I_{z,lb}$) are determined based on the power requirement patterns and the SoC differences between batteries. E_z is the amount of energy transferred for SoC-balancing.

Alg. 4 determines the current ranges for energy transfer to balance SoC while considering the time period (T_z), the remaining energy difference (E_z), and the power requirement pattern (I_{avg}, I_{std}). We search for $I_{z,ub}$ to achieve the battery SoC-balancing ($E_{tr} = E_z$) within the required time period (T_z). Then, the amount of energy transferred between batteries can be calculated according to Eq. (4).

Algorithm 4 Find bounds for SoC-balancing

1: **procedure** $[I_{z,ub}, I_{z,lb}]$ = FINDBOUNDSOC($T_z, E_z, I_{avg}, I_{std}$)
2: **for** $I_{z,ub} = 0; I_{z,ub} < I_{avg} + 2I_{std}; I_{z,ub} = I_{z,ub} + \frac{I_{std}}{20}$ **do**
3: $I_{z,lb} = -I_{z,ub}$
4: **if** $E_{tr}(T_z, I_{z,ub}, I_{z,lb}) < E_z$ **then**
5: Break;
6: **end if**
7: **end for**
8: **return** $[I_{ub}, I_{lb}]$
9: **end procedure**

$$
\begin{aligned}
E_{tr} &= \int_0^{T_z} P_{bal}(t)dt \\
&= T_z \int_0^{I_{z,ub}} V_o(I_{z,ub} - i)\mathrm{PDF}(i)di \\
&+ T_z \int_{I_{z,lb}}^{0} V_o(i - I_{z,lb})\mathrm{PDF}(i)di \\
&= T_z V_o \Big[I_{z,ub} \int_0^{I_{z,ub}} \mathrm{PDF}(i)di - \int_0^{I_{z,ub}} i\mathrm{PDF}(i)di \\
&+ \int_{I_{z,lb}}^{0} i\mathrm{PDF}(i)di - I_{z,lb} \int_{I_{z,lb}}^{0} \mathrm{PDF}(i)di \Big] \\
&= T_z V_o \Big[I_{z,ub}[\mathrm{CDF}(I_{z,ub}) - \mathrm{CDF}(0)] \\
&- [I_{std}^2(\mathrm{PDF}(0) - \mathrm{PDF}(I_{z,ub})) + I_{avg}(\mathrm{CDF}(I_{z,ub}) - \mathrm{CDF}(0))] \\
&+ [I_{std}^2(\mathrm{PDF}(I_{z,lb}) - \mathrm{PDF}(0)) + I_{avg}(\mathrm{CDF}(0) - \mathrm{CDF}(I_{z,lb}))] \\
&- I_{z,lb}[\mathrm{CDF}(0) - \mathrm{CDF}(I_{z,lb})] \Big] \qquad (4)
\end{aligned}
$$

V. EVALUATION

We evaluate the proposed current management for peak discharge/charge reduction and SoC-balancing, while focusing on whether or not they meet the goals stated in Section II. We used Li-ion batteries as the energy-dense battery, and Ultra-Capacitors (UCs) as the power-dense battery. The sizes of UCs and batteries are determined by our HESS design approach.

A. Experimental setup

We have built a prototype with wheels, wheel motors, stepper motors, coolers and an HESS, including a pack of lithium-ion batteries and a pack of UCs as shown in Fig. 7. We first determined the sizes of UCs and batteries based on the power requirement analysis. For realistic evaluations, we acquired driving profiles/data from the Air Resources Board (ARB02) and US Environmental Protection Agency (UDDS, SC03, US06) [6]. The UDDS driving cycle is exploited to design the HESS. The system is required to execute user applications, and allocate available resources for their execution. We programmed the applications to operate wheel motors to achieve the driving profiles (UDDS, SC03, US06).

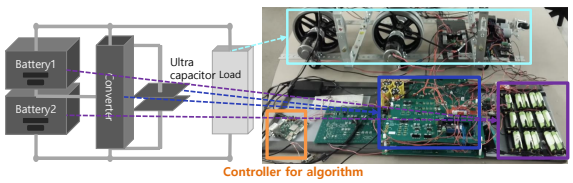

Fig. 7. Our prototype for evaluation

B. Results

For an efficient HESS design whose weight (m_{rq}) is 600 kg, 589 kg of energy-dense battery ($P_e^s = 58W/kg$, $E_e^s = 171Wh/kg$) and 11 kg of power-dense battery ($P_p^s = 10,000w/kg$, $E_e^s = 38Wh/kg$) are selected. To conduct experiments in the lab, we built a small-scale HESS which has similar ratio of energy and power properties to that of the optimized configuration using available energy devices. We could choose 15 Lithium-ion batteries [9] that have 122 Wh of energy capacity and 277.5 W of power capability. Our HESS, also, includes two ultra capacitors [10] that can store 0.81 Wh of energy and 140 W of maximum power in them as shown in Table I.

Parameters	$E_e(Wh)$	$E_p(Wh)$	$P_e(W)$	$P_p(W)$
OPT	100,720	418	34,160	110,000
EXP	122	0.81	277.5	140

TABLE I
OPTIMIZED DESIGN PARAMETERS (OPT) AND EXPERIMENTAL PARAMETERS (EXP)

Fig. 8 shows the current measurements resulting from the peak power reduction control. It shows the current requirements (I_{rq}) with a pattern (I_{avg}, I_{std}) and the discharge/charge current (I_b) from the battery with the determined bounds ($I_{b,ub}, I_{b,lb}$). Fig. 9 plots the results of a SoC-balancing example. When the SoC differences exceed its threshold, the controller starts to regulate the converter switches to transfer charges for SoC-balancing. To protect batteries from large discharge/charge stresses due to SoC-balancing, the charge transfer operations take place only when the current requirements are within the current bounds ($I_{z,lb} < I_{rq} < I_{z,ub}$).

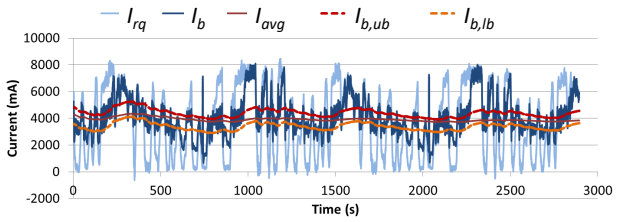

Fig. 8. Example of the proposed power buffering for peak power reduction. Battery and buffer currents are controlled by the algorithm in Fig 5. Upper and lower current bounds are determined by Alg. 3 and Eq. (3)

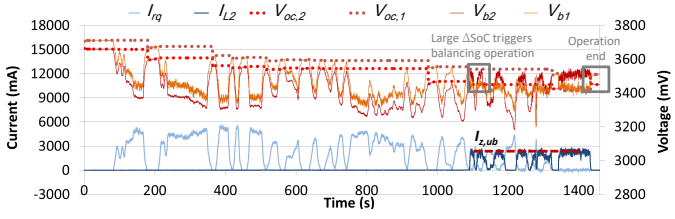

Fig. 9. Example of the proposed SoC-balancing. Battery and buffer currents are controlled by the algorithm in Fig 6. Upper and lower current bounds are determined by Alg. 4 and Eq. (4)

We evaluate the dis/charge stress based on the side reaction rate estimates ($\frac{1}{T}\int a \cdot e^{b\cdot|I_b|}\, dt$) introduced in [8]. Note that

Driving cycle	UDDS	ARB02	SC03	US06
Stress (baseline)	1.44	1.34	1.53	3.21
Stress (our approach)	1.25	1.05	1.33	2.62
Reduction ratio	13.6%	21.8%	13.1%	18.2%

TABLE II
DIS/CHARGE STRESS ($\frac{1}{T}\int a \cdot e^{b\cdot|I_b|}\, dt$) UNDER THE PROPOSED PEAK POWER REDUCTION AND THE BASELINE

T is an operation period and, a and b can be approximated by parameters including charge transfer coefficients and material/solvent concentrations in [8]. Table II shows the discharge/charge current stresses at different driving cycles. The proposed discharge/charge current management reduces the discharge/charge stress while reducing SoC imbalances at the end of cycle by up to about 21.8%.

VI. CONCLUSION

We have designed a hybrid energy storage system (HESS) and proposed its discharge/charge current management so as to minimize the battery discharge/charge stress and ensure SoC-balancing among battery cells. To adaptively control the discharge/charge rate, we have also proposed an algorithm for determining the discharge/charge rate while considering the current requirement pattern and the SoCs of each energy storage component. We have validated the algorithm with the optimized HESS-powered prototype running realistic applications, demonstrating peak current reduction and SoC-balancing. In future, we would like to develop a design framework for general large-scale energy storage systems.

ACKNOWLEDGEMENT

The work reported in this paper was supported by NSF under Grants CNS-1446117 and 1739577.

REFERENCES

[1] R. Kaiser, "Optimized battery-management system to improve storage lifetime in renewable energy systems," *Journal of Power Sources*, vol. 168, no. 1, pp. 58 – 65, 2007.

[2] S. Park, Y. Kim, and N. Chang, "Hybrid energy storage systems and battery management for electric vehicles," in *Design Automation Conference (DAC), 2013 50th ACM/EDAC/IEEE*, May 2013, pp. 1–6.

[3] Z. Song, H. Hofmann, J. Li, X. Han, and M. Ouyang, "Optimization for a hybrid energy storage system in electric vehicles using dynamic programing approach," *Applied Energy*, vol. 139, pp. 151 – 162, 2015.

[4] S. M. Lukic, S. G. Wirasingha, F. Rodriguez, J. Cao, and A. Emadi, "Power management of an ultracapacitor/battery hybrid energy storage system in an hev," in *2006 IEEE Vehicle Power and Propulsion Conference*, Sep. 2006, pp. 1–6.

[5] S. W. Moore and P. J. Schneider, "A review of cell equalization methods for lithium ion and lithium polymer battery systems," in *SAE Technical Paper*. SAE International, 03 2001.

[6] Dynamometer drive schedules. Available: https://www.epa.gov/vehicle-and-fuel-emissions-testing/dynamometer-drive-schedules

[7] Y. Tang, Y. Zhang, W. Li, B. Ma, and X. Chen, "Rational material design for ultrafast rechargeable lithium-ion batteries," *Chem. Soc. Rev.*, vol. 44, pp. 5926–5940, 2015.

[8] X. Lin, J. Park, L. Liu, Y. Lee, A. M. Sastry, and W. Lu, "A comprehensive capacity fade model and analysis for li-ion batteries," *Journal of The Electrochemical Society*, vol. 160, no. 10, pp. A1701–A1710, 2013.

[9] TENERGY. Tenergy 3.7v 2200mah lithium-ion 18650 flat top rechargeable battery with pcb. http://www.tenergy.com/30015.

[10] EATON. Snap-in cylindrical supercapacitors. https://www.eaton.com/us/en-us/catalog/electronic-components/xv-supercapacitor.html.